IOSR Journal of Electrical and Electronics Engineering (IOSR-JEEE)
e-ISSN: 2278-1676,p-ISSN: 2320-3331, Volume 7, Issue 6 (Sep. - Oct. 2013), PP 01-07
www.iosrjournals.org

The study of semiconductor layer effect on underground cables with Time Domain Reflectometry (TDR)

Rodrigo Paludo[1], Guilherme Cunha da Silva[2], Vitoldo Swinka Filho[3]
[1,2and 3] (Department of Materials, Universidade Federal do Paraná, Brasil)

Abstract: *Time Domain Reflectometry is a technique used for fault location and partial discharge analysis in underground electric distribution cables. The technique is based on the analysis of the propagation of short electric pulses. In underground cables, semiconductor layer properties and degradation cause perturbations in the signal wave shape. These perturbations complicate the interpretation of reflectograms and, as a consequence, fault location. This work presents a circuit model of distributed elements that includes the electrical resistance of the semiconductor layers. The results of computer simulations using the proposed model are compared with measurements in new and aged XLPE cables. This comparison shows that the proposed model can represent the phenomena satisfactorily.*
Keywords : *Underground cables, Simulation of Time Domain Reflectometry, Attenuation spectrum.*

I. INTRODUCTION

Rapid fault localization in underground cables reduces grid maintenance time and, as a consequence, reduces service interruption time. In this context, Time Domain Reflectometry (TDR) is an appropriate technique to quickly find a fault by analyzing the behavior of short electric pulses propagating in the cable. The electrical pulses propagate along the cable and can be absorbed or reflected as a result of changes in the characteristic impedance [1].

Measurements in aged cables show changes in the pulse behavior that make TDR analysis difficult.
In this work, the semiconductor layer's electric resistance is considered in explaining the pulse attenuation and dispersion during propagation in new and aged cables, using cable measurements and computational simulations.

II. MATERIALS AND METHODS

The comparison was performed using XLPE (cross-linked polyethylene) insulated cables, both new and aged, whose characteristics are shown in Table 1. The cable labeled XLPE-A was manufactured in the 1970s and was removed from operation. The cable labeled XLPE-N is a new cable that has not been used in operation.

Table 1 – Cable characteristics.

Cables	XLPE-N (new)	XLPE-A (aged)
Internal diameter (conductor)	8 mm	9 mm
External diameter (insulation)	17.5 mm	19 mm
Internal semiconductor layer thickness	1.2 mm	0.6 mm
External semiconductor layer thickness	1.5 mm	0.5 mm
Characteristic Impedance	33 Ω	36 Ω
Cable length	67 m	33 m
Material of the internal conductor	Aluminum	
Aluminum conductivity	$59.6x10^{6}\ \Omega m^{-1}$	
Dielectric	XLPE	
XLPE conductivity	$\cong 10^{-15}\ \Omega m^{-1}$	
XLPE relative permittivity	2.4	
Voltage class	12/20 kV	
Vacuum magnetic permeability	$4\pi\, x 10^{-7}\ Tm/A$	
Relative magnetic permeability of the conductor	1	
Vacuum electric permittivity	$8.85x10^{-12}\ C^2/Nm^2$	
Frequency	25 MHz	

To perform TDR, an oscilloscope was used with an acquisition rate of 1 GS/s, and the pulses were generated with a digital function generator. Fig. 1 shows the classic model of a distributed circuit element [2, 3].

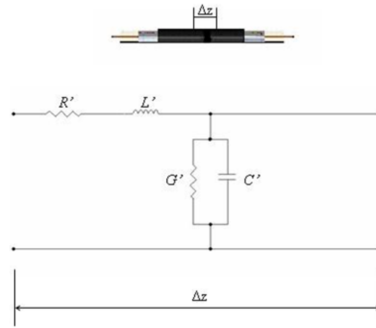

Figure 1 – Classic model of a distributed element.

The electrical characteristics for a coaxial line are given by [2, 3]:

$$R' = \frac{R_s}{2.\pi}\left(\frac{1}{a}+\frac{1}{b}\right) \quad (1)$$

$$L' = \frac{\mu}{2\pi}\ln\left(\frac{b}{a}\right) \quad (2)$$

$$G' = \frac{2\pi\sigma}{\ln\left(\frac{b}{a}\right)} \quad (3)$$

$$C' = \frac{2\pi\varepsilon}{\ln\left(\frac{b}{a}\right)} \quad (4)$$

where

$R' \rightarrow$ *Resistance per unit length* $[\Omega / m]$;
$L' \rightarrow$ *Inductance per unit length* $[H / m]$;
$G' \rightarrow$ *Conductance per unit length* $[S / m]$;
$C' \rightarrow$ *Capacitance per unit length* $[F / m]$;
$a \rightarrow$ *Internal conductor radius [m];*
$b \rightarrow$ *External conductor radius [m];*
$\mu \rightarrow$ *Dielectric magnetic permeability* $[T.m / A]$;
$\sigma \rightarrow$ *Dielectric conductivity* $[\Omega.m^{-1}]$; *and*
$\varepsilon \rightarrow$ *Dielectric electric permittivity* $[C^2 / N.m^2]$.

The resistance per unit length of the cable is determined using the intrinsic resistance (Rs), i.e., the skin resistance of the conductor [2, 3],

$$R_s = \sqrt{\frac{\pi.f.\mu_c}{\sigma_c}} \quad (5)$$

where

$f \rightarrow$ *Frequency* $[Hz]$;
$\mu_c \rightarrow$ *Conductor magnetic permeability* $[T.m / A]$; *and*
$\sigma_c \rightarrow$ *Conductor conductivity* $[\Omega.m^{-1}]$.

III. RESULTS AND DISCUSSION

The Fig. 2 shows the schematic diagram of the experimental setup for TDR.

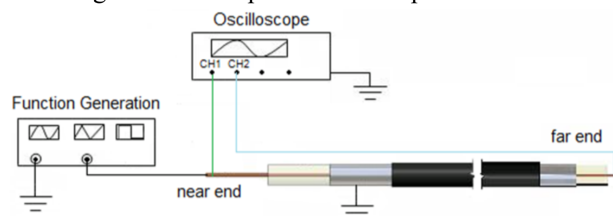

Figure 2 – Experimental layout for TDR.

Channel 2 from the oscilloscope was connected to the far end of the cable.

3.1 XLPE-N Cable

Using the values from Table 1 and equations (1 - 5), the values of the parameters per unit of cable length were obtained and are shown in Table 2.

Table 2 – Parameter values of the XLPE-N cable.

Parameters of the cable	Values	Units
R'	$7.27x10^{-2}$	Ω / m
L'	$1.73x10^{-7}$	H / m
C'	$1.54x10^{-10}$	F / m
G'	$7.26x10^{-15}$	S / m

Fig. 3 shows the circuit diagram for the XLPE-N cable where two elements were used for one meter of length.

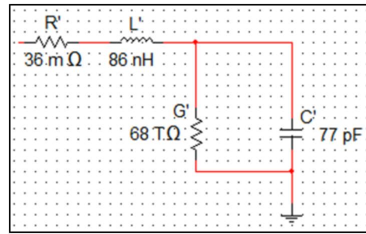

Figure 3 – Schematic circuit showing an element used in the simulation of the XLPE-N cable.

The characteristic impedance of the cable is calculated using equation (6) [3], and the value obtained is used to link the impedance of the function generator with the cable.

$$Z_0 = \sqrt{\frac{R' + jwL'}{G' + jwC'}} \qquad (6)$$

$$Z_0 = (33.42 - j0.045)\ \Omega$$

Fig. 4 shows the result of the simulation for the XLPE-N cable with an open far end.

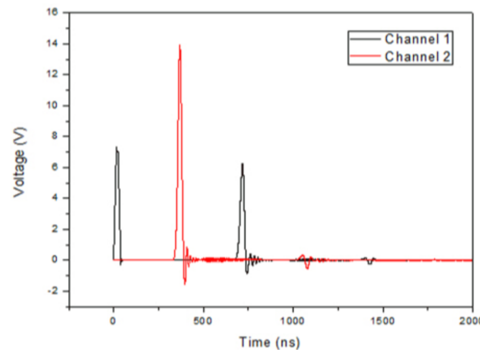

Figure 4 – Simulation reflectogram of the XLPE-N cable with an open far end.

Fig. 5 shows the reflectogram of the XLPE-N cable measured in the laboratory. Comparing Fig. 5 with Fig. 4, the agreement between the simulation and lab measurements can be observed.

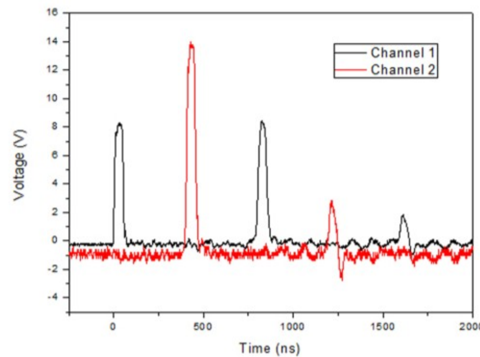

Figure 5 – Experimental reflectogram of the XLPE-N cable with an open far end.

Fig. 6 shows the results of a simulation with the far end short circuited, where the reflected pulse presents a negative polarity.

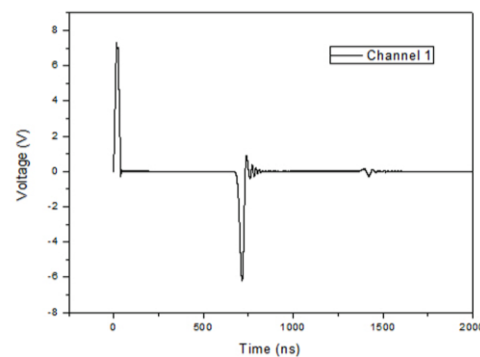

Figure 6 – Simulation reflectogram of the XLPE-N cable in short circuit.

The experimentally obtained reflectogram with the cable in short circuit is shown in Fig. 7.

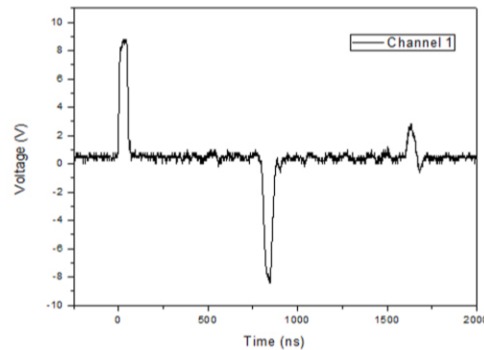

Figure 7 – Experimental reflectogram of the XLPE-N cable in short circuit.

Comparing the simulated and experimental graphs, it can be observed that the simulation results are consistent with the data obtained experimentally from the XLPE-N cable.

3.2. XLPE-A Cable

The same procedure used for the XLPE-N cable was adopted for the XLPE-A cable. The values of the calculated parameters per unit length of cable are presented in Table 3.

Table 3 – Parameters values of cable XLPE-A.

Parameters of cable	Values	Units
R'	$6.33x10^{-2}$	Ω / m
L'	$1.87x10^{-7}$	H / m
C'	$1.42x10^{-10}$	F / m
G'	$6.69x10^{-15}$	S / m

The circuit diagram for the XLPE-A cable is shown in Fig. 8, where two elements were used for one meter of length.

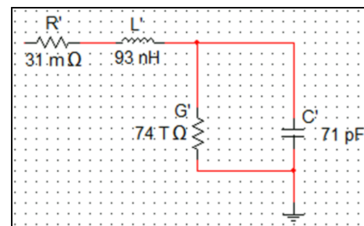

Figure 8 – Schematic circuit showing an element used in the simulation of the XLPE-A cable.

The value of the characteristic impedance [4] that was calculated for the aged cable is:

$$Z_0 = (36.28 - j0.0409)\ \Omega$$

Fig. 9 shows the simulated reflectogram of the XLPE-A cable in an open circuit.

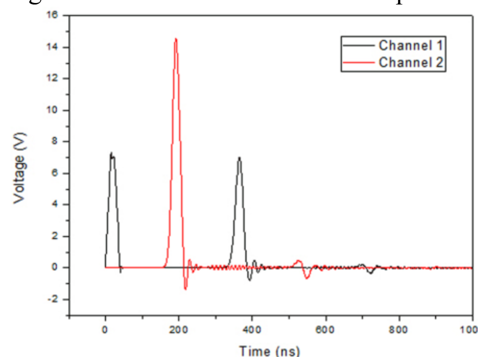

Figure 9 – Simulation reflectogram of the XLPE-A cable in open far end.

Fig. 10 shows the reflectogram of the XLPE-A cable obtained with the same arrangement as the reflectogram presented in Figure 5. In this case, the simulated and experimental reflectograms do not agree, unlike with the XLPE-N cable.

The velocity of pulse propagation in the XLPE-A cable was calculated using equation (7) [4, 5], giving a value of $195\ m/\mu s$.

$$v_p = \frac{1}{\sqrt{\mu.\varepsilon}} \tag{7}$$

With this value of the velocity, the pulse should be observed at the far end of the cable with 169 *ns* of delay, shown by an arrow in Fig. 10.

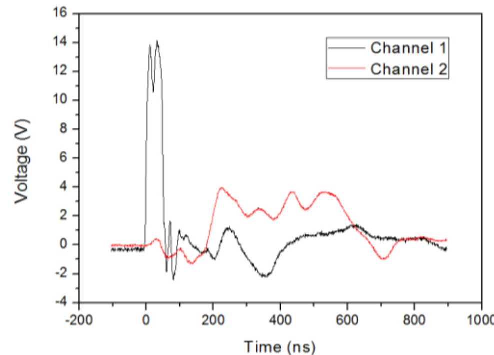

Figure 10 – Experimental reflectogram of the XLPE-A cable with an open far end.

Because the theory for transmission lines [6, 7] was applied equally to the two kinds of the cables (new and aged), the reflectograms should have the same waveform. However, Fig. 9 and Fig. 10 show that the measured behavior of the cable disagrees with that predicted by the classical model of distributed elements. Therefore, work was directed toward explaining this phenomenon.

IV. MODEL OF DISTRIBUTED ELEMENTS PROPOSED

The first hypothesis to explain the observed phenomenon in the aged cable was related to the resistivity of the semiconductor layers and the conductance of the dielectric. The comparison value of resistivity in Table 4, between aged (XLPE-A1 and XLPE-A2) and new (XLPE-N) cables, show that for outer layer the orders of magnitude are equal. For the inner layer the aged cable show lower value than the new cable and however this hypothesis was discarded.

Table 4 – Values of resistivity measure.

Semiconductor layer	XLPE-A1	XLPE-A2	XLPE-N
Inner	5.21×10^{-3}	3.77×10^{-3}	3.94×10^{-1}
Outer	2.77×10^{-2}	2.3×10^{-2}	5.18×10^{-2}

The hypothesis of change in the electrical conductance was evaluated by simulation using values in the range of 10^{-15} S to 10^{-3} S and this change was not able to explain the effect of the Fig. 10. A new model was proposed in which the semiconductor layers are represented by resistances R_i (resistance of inner semiconductor layer) and R_o (resistance of outer semiconductor layer) connected in series with the capacitance and conductance of the distributed-element model, as shown in Fig. 11. In this proposed model, the hypothesis states that there are mechanisms in the semiconductor layers that are activated by the aging of the cable, and this can change the way that the pulses propagate in the cable. These changes make the cables become dissipative and dispersive [7, 11].

The waveform signal, shown in Fig. 10, was used as a measure to relate the simulations to a resistance value that is appropriate for the representation of the semiconductor layers.

The simulated resistance $(R_i + R_o)$ was varied from 20 Ω to 1 kΩ to find a value where the simulated reflectogram matched the experimental reflectogram in Fig. 10.

As the value of the resistance was increased, the simulated reflectogram more closely approximated the experimental reflectogram.

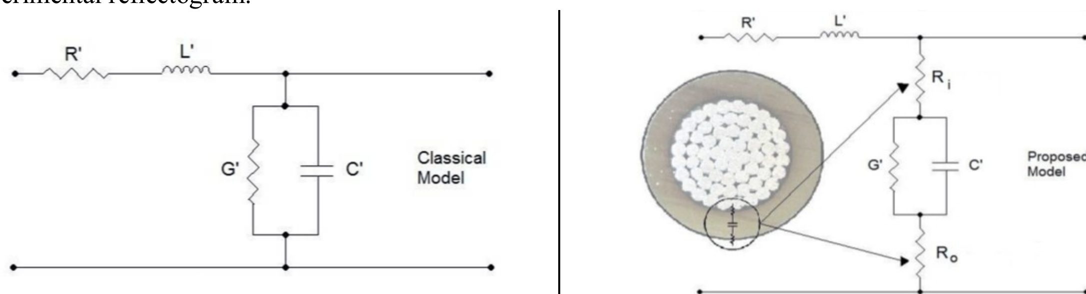

Figure 11 – Schematic drawing of the classical model and the proposed model.

The criterion used for selecting a value of resistance was to compare the ratio of the amplitudes of input pulse with the far end pulse. As the reflectogram in Fig. 10 shows, the rate is approximately 3.5 times, and this value was taken as a reference. The resistance value that produced the simulation results closest to the experimental results for the XLPE-A cable was 100 Ω.

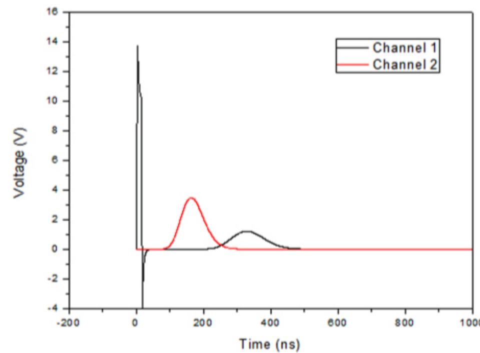

Figure 12 – Simulated reflectogram of an XLPE-A cable with an open far end proposed model and a semiconductor layer resistance of 100 Ω.

The resistivity measurements of the semiconductor layers showed that the intrinsic resistance of the XLPE-A cable is not responsible for the change in the waveform. This phenomenon, shown in fig. 10, was attributed to the coupling of the electrical resistance of the semiconductor layers with other parts of the cable.

In cables that are more than 25 years old, there are regions of oxidation in the semiconductor layers (outer and inner), which can be observed in Fig. 13.

Figure 13 – XLPE cables (aged on the left and new on the right).

It was observed that the tape in the semiconductor layer of the XLPE-A cable has a low intrinsic resistance value per meter; however, the layer is positioned between the electromagnetic shielding and the dielectric. This layer undergoes an increase in coupling resistance due to oxidation caused by the humidity that occur during the cable's lifetime. This oxidation is not observed in the new cable.

The energy dissipation factor of the pulse was studied using simulations with different values of resistance representing the semiconductor layers of the cable. This study was performed by comparing the ratio between the energy of a pulse position of the cable and the pulse energy injected into the cable. The results of this study are shown in Fig. 14.

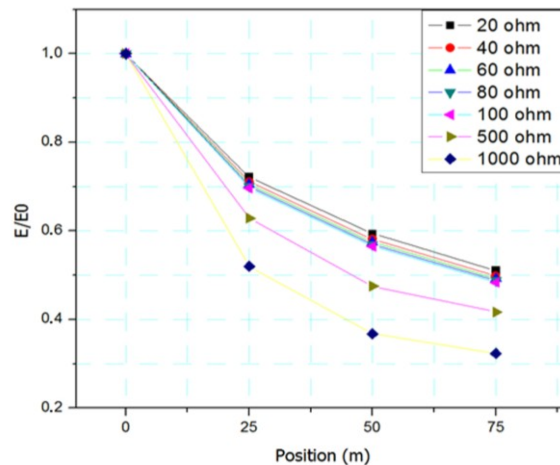

Figure 14 – Comparison of the attenuation along the cable with different resistance values.

In Fig. 14, it can be observed that the ratio E/E0 decreases with increasing semiconductor layer resistance. The dissipative behavior for different cable lengths is shown in Fig. 15. This graph was obtained by simulating the proposed model of the cable with the electrical resistance of the semiconductor layers equal to 100 Ω. The graph shows the spectrum of attenuation, which is a characteristic of the cable.

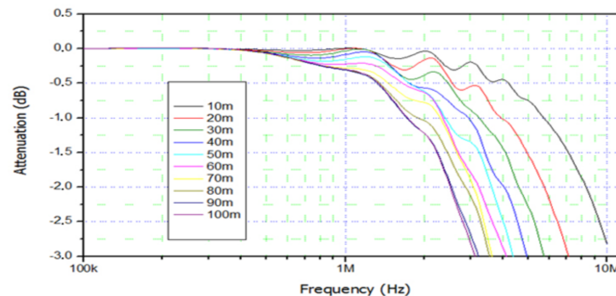

Figure 15 – Attenuation spectrum simulated for a cable with semiconductor layer resistance of 100 Ω.

What can be concluded from the attenuation spectrum of the cable, from 100 kHz to 10 MHz, is that as the length of the cable increases, the value of the cutoff frequency decreases. For example, at 10 meters from the beginning of the cable, the cutoff frequency is approximately 10 MHz, while at 100 meters from the beginning of the cable, the cutoff frequency decreases to approximately 5 MHz. Therefore, it can be observed that the attenuation constant of the cable is related to the pulse frequency.

V. CONCLUSION

The results of the reflectometry performed on aged cable did not agree with the simulation results using the classical model of distributed elements.

The proposed model produces better agreement with the results of reflectometry that were obtained from the aged cables. The proposed model introduces a resistance to represent the semiconductor layers at the inner and outer surfaces of the XPLE dielectric. This resistance can be associated with the degradation mechanisms in these layers.

The results of the calculations of the resistance per unit length of material from the semiconductor layers, which was performed using the results of the measured electric resistivity, show that although the values of resistance are small, they have a significant contribution in this phenomenon. Predominantly, the resistance is caused by the mechanisms of degradation, such as oxidation. This is confirmed by the results of simulations and reflectometry made on the new cable, which does not show the dispersive behavior.

The results of simulations with the proposed model showed that the attenuation increases proportionally with the resistance presented by the semiconductor layers and the degradation mechanisms. Additionally, it was observed that the attenuation is a function of frequency, which does not occur in the classical model.

REFERENCES

[1] V. DUBICKAS, H. EDIN and R. PAPAZYAN, "Cables Diagnostics with On-Voltage Time Domain Reflectometry," Royal Institute of Technology, 2006.

[2] D. k. CHENG, "Field and Wave Electromagnetics," Second Edition, Addison-Wesley Publishing Company, Boston, pp. 370 - 428, 1989.

[3] F. T. ULABY, E. MICHIELSSEN and U. RAVAIOLI, "Fundamentals of Applied Electromagnetics," Sixth Edition, Pearson, University of Michigan, pp. 67 - 131, 1994.

[4] P. WAGENAARS, P.A.A.F Wouters, P.C.J.M. Van Der Wielen and E.F. Steennis, "Estimation of Transmission Line Parameters for Single-core XLPE Cables," International Conference on CMD, pp. 1132 – 1135, Beijing, 2008.

[5] M. E. KOWALSKI, "A Simple and Efficient Computational Approach to Chafed Cable Time-Domain Reflectometry Signature Prediction," Stinger Ghaffarian Technologies (SGT), Inc. NASA Ames Research Center, 2008.

[6] V. DUBICKAS, "Development of On-line Diagnostic Methods for Medium Voltage XLPE Power Cables" Doctoral Thesis, Stockholm, Sweden 2009.

[7] R. PALUDO, "Refletometria no Domínio do Tempo: Análise das Camadas Semicondutoras de Cabos Isolados," Dissertation of Master, Curitiba 2009.

[8] R. PAPAZYAN and R. ERIKSSON, "Calibration for Time Domain Propagation Constant Measurements on Power Cables," IEEE Transactions on Instrumentation and Measurement, vol. 52, pp. 415 – 418, 2003.

[9] R. HEINRICH, S. BONISCH, D. POMMERENKE, R. JOBAVA and W. KALKNER, "Broadband Measurement of the Conductivity and the Permittivity of Semiconducting Materials in High Voltage XLPE Cables," **Eighth International Conference on (IEE Conf. Publ. No. 473),** pp. 212 – 217, 2000.

[10] G. MUGALA, R. ERIKSSON and P. Petersson, "Comparing Two Measurements Techniques for High Frequency Characterization of Power Cable Semi conducting and Insulating Materials," IEEE Trans. on Dielectrics and Electrical Insulation, vol. 13, pp. 712 – 716, 2006.

[11] O. HIO NAM, T. R. BLACKBURN and B. T. PHUNG, "The Effect of Insulation Loss and Semi-Conducting Layers on Pulse Propagation Behavior of Power Cables," **Power Engineering Conference, pp. 1 – 5, Australasian Universities**, 2007.